Molecular Plant Pathology

MOLECULAR PLANT PATHOLOGY (2010) **11**(5), 625–640 DOI: 10.1111/J.1364-3703.2010.00633.X

# Cellular and transcriptional responses of wheat during compatible and incompatible race-specific interactions with *Puccinia striiformis* f. sp. *tritici*

TOLGA O. BOZKURT[1,2,†], GRAHAM R.D. MCGRANN[2], RUTH MACCORMACK[2], LESLEY A. BOYD[2] AND MAHINUR S. AKKAYA[1,*]

[1]*Middle East Technical University, Department of Chemistry, Biochemistry and Biotechnology Programs, Ankara, TR-06531, Turkey*
[2]*John Innes Centre, Department of Disease and Stress Biology, Colney Lane, Norwich NR4 7UH, UK*

## SUMMARY

The initial stages of *Puccinia striiformis* f. sp. *tritici* (the causal agent of yellow rust in wheat) infection triggered a hypersensitive cell death (HCD) response in both compatible and *Yr1*-mediated incompatible interactions, although the response was earlier and more extensive in the incompatible interaction. Later stages of fungal development were only associated with an HCD response in the incompatible interaction, the HCD response being effectively suppressed in the compatible interaction. Cell autofluorescence was seen in mesophyll cells in direct contact with fungal infection hyphae (primary HCD) and in adjacent mesophyll cells (secondary HCD), indicating the activation of cell-to-cell signalling. Microarray analysis identified a number of defence-related transcripts implicated in *Yr1*-mediated resistance, including classical pathogenesis-related (*PR*) transcripts and genes involved in plant cell defence responses, such as the oxidative burst and cell wall fortification. A quantitative reverse transcriptase-polymerase chain reaction time course analysis identified a number of defence-related genes, including *PR2*, *PR4*, *PR9*, *PR10* and *WIR1* transcripts, associated with the latter stages of *Yr1*-mediated resistance. A meta-analysis comparison of the *Yr1*-regulated transcriptome with the resistance transcriptomes of the race-specific resistance gene *Yr5* and the race-nonspecific adult plant resistance gene *Yr39* indicated limited transcript commonality. Common transcripts were largely confined to classic *PR* and defence-related genes.

## INTRODUCTION

*Puccinia striiformis* f. sp. *tritici* is an obligate biotrophic fungus and the causal agent of yellow rust (also known as stripe rust) of wheat (*Triticum aestivum* L.). Yellow rust is an economically important foliar disease, particularly prevalent in temperate and maritime wheat-growing regions, resulting in yield losses in the range of 10%–70% where susceptible wheat varieties are grown (Boyd, 2005; Chen, 2005). The disease is generally controlled through a combination of resistance (*R*) gene deployment and fungicide application. Major race-specific *R* genes have been a valuable weapon in the wheat breeders' armoury. However, the effectiveness of *R* genes tends to be short lived because of virulence changes in the pathogen population (Bayles *et al*., 2000). The race-specific *R* gene *Yr1* was identified by Lupton and Macer (1962) and has been deployed worldwide. Consequently, virulence to *Yr1* is common in many parts of the world, including Europe and the Far East (McIntosh *et al*., 1995). However, in Turkey, a major producer and exporter of wheat where yellow rust is a serious disease, *Yr1* is still effective (personal communication with the officials at 'Tarla Bitkileri Merkez Arastirma Enstitusu', Ankara, Turkey).

The infection stages of the asexual life cycle of *P. striiformis* f. sp. *tritici* are well defined. Airborne urediniospores germinate on the plant surface and enter the plant through stomatal openings. A substomatal vesicle forms within the stomatal cavity, from which three infection hyphae grow. At the point of contact between an infection hypha and a host mesophyll cell, a haustorial mother cell differentiates. An infection peg develops, breaching the mesophyll cell wall and establishing a haustorium inside the living mesophyll cell. Further colonization occurs through the development of intercellular runner hyphae which grow throughout the leaf, producing further haustoria. By 14 days after inoculation, the asexual life cycle is complete and urediniospore-bearing upedicels erupt through the leaf epidermis, forming the characteristic yellow pustules (Cartwright and Russell, 1981; Garrood, 2001; Mares, 1979; Mares and Cousen, 1977). However, little is known about the processes involved in the perturbation of this infection cycle, with different yellow rust resistance genes appearing to disrupt the infection process at

*Correspondence: Email: akkayams@metu.edu.tr
†*Present address*: The Sainsbury Laboratory, John Innes Centre, Norwich NR4 7UH, UK.

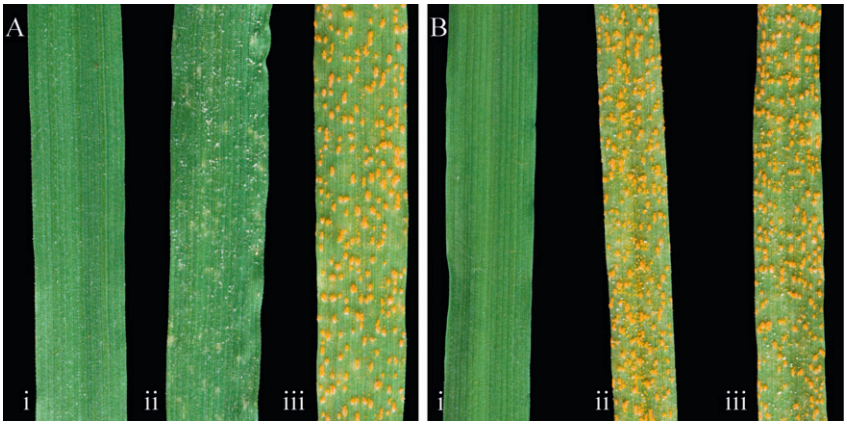


**Fig. 1** *Puccinia striiformis* f. sp. *tritici* inoculations. Yellow rust infection phenotypes 14 days after inoculation on Avocet*6/*Yr1* (A) and Avocet S (B) inoculated with mock (i), the *Yr1*-avirulent race 232E137 (ii) and the *Yr1*-virulent race 169E136 (iii). The incompatible interaction (Aii) shows small necrotic flecks, whereas the three compatible interactions (Aiii, Bii and Biii) show yellow rust pustules.

different stages in the pathogen's development (Jagger, 2009; Melichar *et al*., 2008; Moldenhauer *et al*., 2006, 2008).

A better understanding of the cellular and molecular mechanisms behind race-specific resistance may allow for the more effective deployment of these *R* genes to achieve durable resistance strategies (Boyd, 2005). Early plant defence responses, triggered by the recognition of conserved pathogen-associated molecular patterns (PAMPs), are collectively referred to as PAMP-triggered immunity (PTI; Zipfel, 2008). Subsequently, *R* gene-mediated responses are triggered by the recognition of specific, pathogen-derived effector molecules, termed avirulence factors. This effector-triggered immunity (ETI) is considered to result in accelerated and stronger defence responses (Jones and Dangl, 2006).

A global picture of the reprogramming of the transcriptome that occurs during host compatible and incompatible interactions in cereals can now be obtained using array technologies. In cereals, changes in the transcriptome produced by a number of pathogens, including those causing yellow and leaf rust in wheat (Bolton *et al*., 2008; Coram *et al*., 2008a, b; Hulbert *et al*., 2007), *Magnaporthe* in wheat and rice (Tufan *et al*., 2009; Vergne *et al*., 2007), *Blumeria graminis* (Caldo *et al*., 2004, 2006) and *Polymyxa* (McGrann *et al*., 2009) infection in barley, and towards ToxA from *Pyrenophora tritici-repentes* in wheat (Adhikari *et al*., 2009), have highlighted the transcripts induced specifically by each *R* gene-mediated interaction, as well as those induced in common during incompatible and compatible plant–pathogen interactions.

In this study, we have investigated the histopathological and transcriptional changes that occur in wheat in response to *P. striiformis* f. sp. *tritici* isolates differing in their virulence for *Yr1*. A comparative analysis of the changes in the transcriptome mediated by *Yr1* was carried out with the transcriptome profiles of other published wheat yellow rust resistance genes. Possible isolate-specific effects were subsequently examined by including, in the histopathological analysis, a compatible, near-isogenic wheat genotype differing only at the *Yr1* locus. *Puccinia striiformis* f. sp. *tritici* development and the plant's cellular responses were examined over a 72-h time course following inoculation.

## RESULTS

### *Puccinia striiformis* f. sp. *tritici* infection phenotypes

Seedlings of Avocet*6/*Yr1* and Avocet S were inoculated with either the *P. striiformis* f. sp. *tritici Yr1*-virulent isolate, race 169E136 (compatible with Avocet*6/Yr1, compatible with Avocet S), or the *Yr1*-avirulent isolate, race 232E137 (incompatible with Avocet*6/*Yr1*, compatible with Avocet S). Yellow rust pustules were observed 14 days post-inoculation (dpi) in all three compatible interactions, whereas, in the incompatible interaction between Avocet*6/*Yr1* and race 232E137, necrotic flecks were seen at 10 dpi. No visible symptoms were observed on mock-inoculated plants of either wheat genotype (Fig. 1).

### *Puccinia striiformis* f. sp. *tritici* development and plant cellular responses

*Puccinia striiformis* f. sp. *tritici* development and subsequent plant responses were monitored over a 72-h time course, taking samples for microscopy and transcriptomic analysis at 6, 12, 24, 48 and 72 h post-inoculation (hpi) in incompatible and compatible interactions with Avocet*6/*Yr1* and Avocet S.

Germ tubes and substomatal vesicles were observed at 6 hpi, and infection hyphae at 12 hpi, in all four wheat genotype–*P. striiformis* f. sp. *tritici* interactions (Fig. 2A). There were no significant differences between each of the four interactions over time, indicating that both isolates developed at similar rates on both wheat genotypes (data not shown). However, significant differences in the ability of each isolate to form infection sites, measured as a percentage of germinated urediniospores that formed substomatal vesicles, were observed (Fig. 3; *F* probability, 0.003).

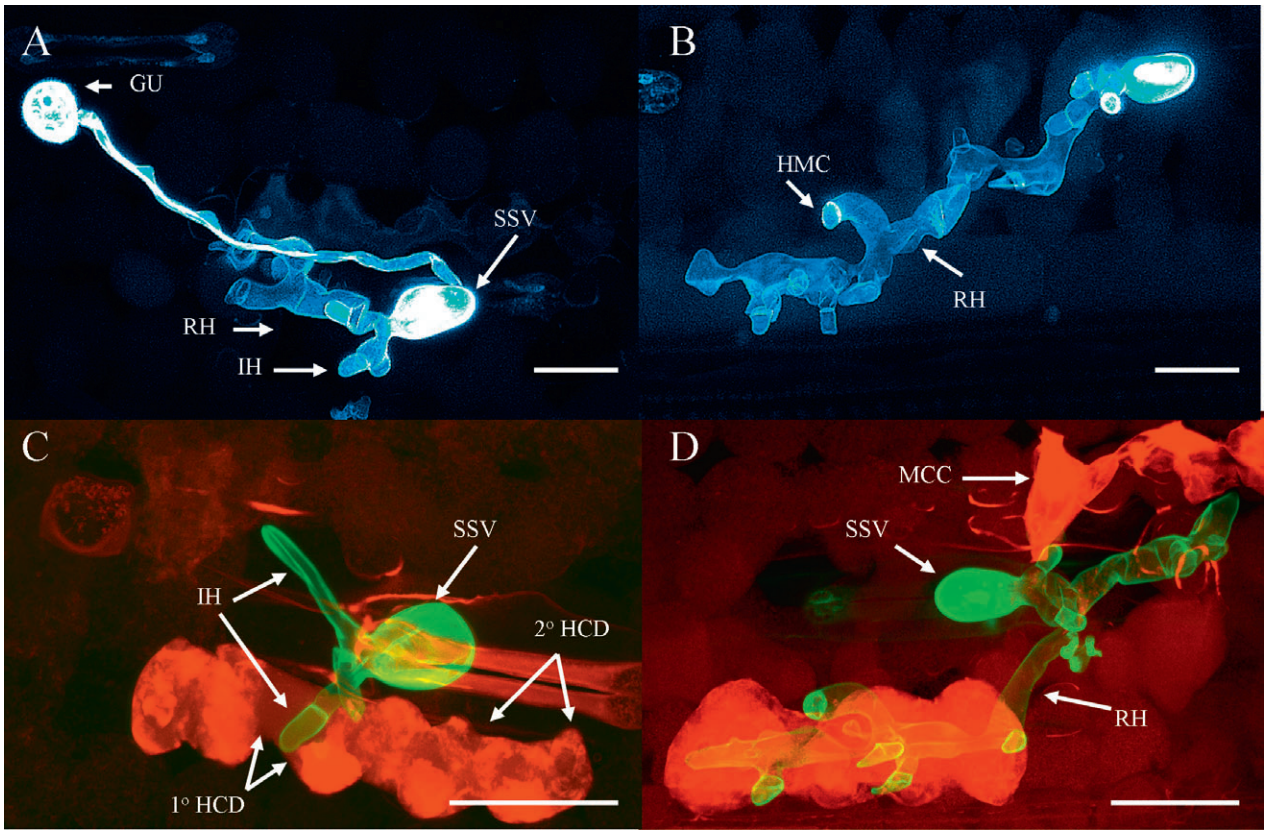


**Fig. 2** *Puccinia striiformis* f. sp. *tritici* development and plant cellular responses. (A) Germinated urediniospore (GU), substomatal vesicle (SSV), primary infection hyphae (IH) and runner hyphae (RH). (B) Haustorial mother cells (HMC) formed along the length of an RH. (C) Mesophyll primary (1° HCD) and secondary (2° HCD) hypersensitive cell death. (D) Mesophyll cell collapse (MCC). All images were taken from the Avocet*6/*Yr1* plus *Yr1*-avirulent isolate 232E137 interaction at 72 hpi. Bars, 50 μm.

The avirulent race 232E137 formed fewer infection sites compared with the virulent race 169E136 (*t*-test probability, 0.004). A genotype–isolate interaction was also observed, with race 232E137 forming fewer infection sites on Avocet S than on Avocet*6/*Yr1* (*t*-test probability, 0.001). Having formed infection sites, the number producing infection hyphae was similar for all four interactions, with 80% of infection sites developing infection hyphae by 24 hpi, rising to 100% by 72 hpi (data not shown).

A hypersensitive cell death (HCD) response towards *P. striiformis* f. sp. *tritici* infection was observed as autofluorescing mesophyll cells (Fig. 2C,D) that eventually underwent granulation and cell collapse (Fig. 2D). HCD was seen in mesophyll cells in direct contact with infection hyphae (primary HCD; Fig. 4A) and in mesophyll cells that were not in direct contact with fungal structures (secondary HCD; Fig. 4B), but adjacent to mesophyll cells undergoing primary HCD. Primary and secondary HCD were observed in both the incompatible interaction and in the three compatible interactions. However, in the incompatible interaction, the proportion of infection sites exhibiting both primary and secondary HCD was significantly greater than in the three compatible interactions (*F* probability, <0.001; *t*-test probability, <0.001). In the incompatible interaction between Avocet*6/*Yr1* and race 232E137, primary HCD was first observed at 24 hpi and, by 48 hpi, over 40% of infection sites exhibited primary HCD. In the three compatible interactions, HCD was slower to appear and involved fewer mesophyll cells. By 48 hpi, secondary HCD was observed in all four wheat genotype–isolate interactions (Fig. 4B).

Runner hyphae (Fig. 2B) were observed at 24 hpi in the compatible interaction between Avocet S and race 169E136 and in all interactions by 48 hpi (Fig. 5A). The number of runner hyphae increased markedly by 72 hpi in all three compatible interactions, with 70%–90% of infection sites having developed runner hyphae by this time point (Fig. 5A). Significantly fewer runner hyphae were produced by infection sites in the incompatible interaction at both 48 and 72 hpi (*t*-test probabilities, 0.01–0.001). Runner hyphae associated with HCD were seen in the incompatible interaction from 48 hpi onwards (Fig. 5B). A small percentage of infection sites in the compatible interaction between Avocet*6/*Yr1* and the virulent race 169E136 exhibited

 

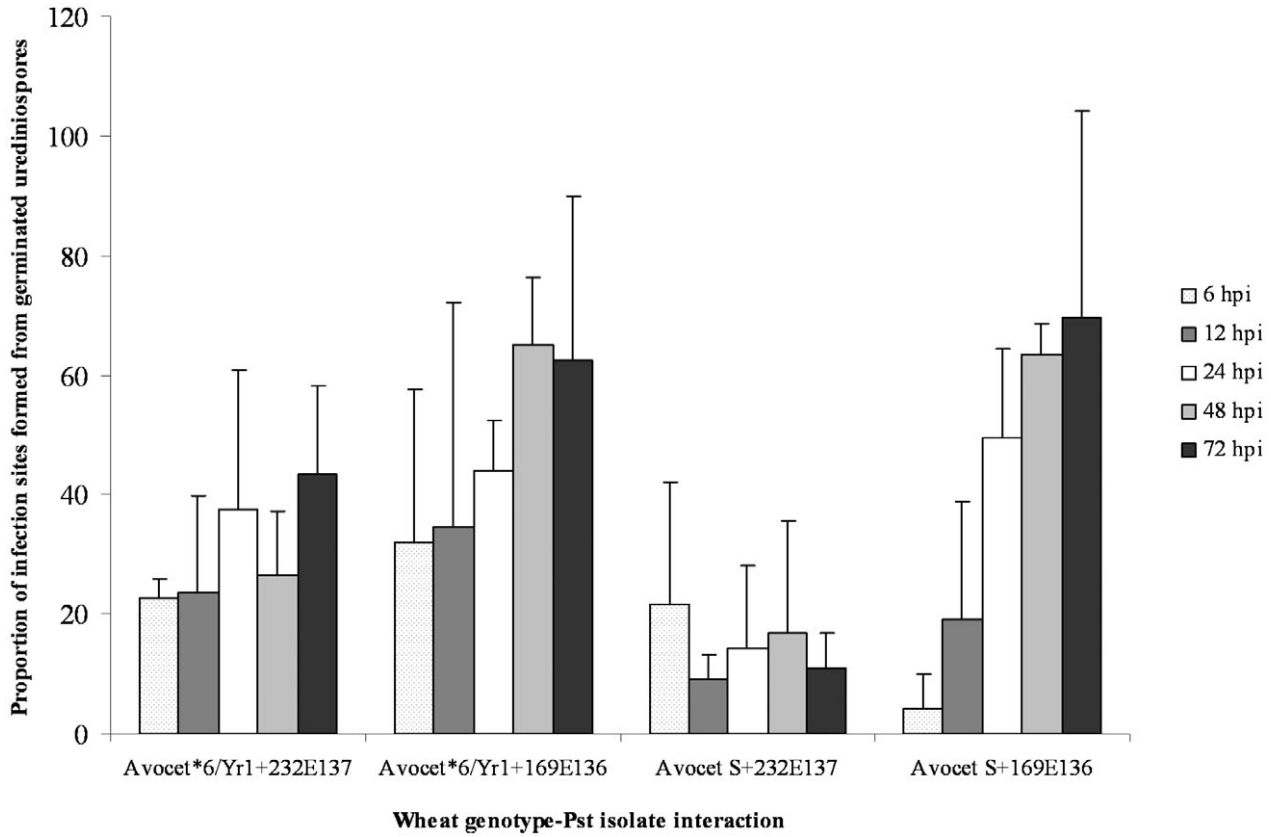


**Fig. 3** *Puccinia striiformis* f. sp. *tritici* (Pst) infection sites. The number of infection sites formed as a percentage of the number of germinated urediniospores is shown over a 72-h time course for the *Yr1*-avirulent isolate 232E137 and the *Yr1*-virulent isolate 169E136 on Avocet*6/*Yr1* and Avocet S.

runner hyphae associated with HCD; however, neither of the Avocet S–*P. striiformis* f. sp. *tritici* compatible interactions produced infection sites in which the runner hyphae were associated with HCD (F probability, <0.001; *t*-test probability, <0.001; Fig. 5B).

## Wheat GeneChip transcriptome analysis of *Yr1* incompatible and compatible interactions

Transcript levels were assessed relative to mock-inoculated controls in incompatible and compatible interactions between Avocet*6/*Yr1* and *P. striiformis* f. sp. *tritici* isolates 232E137 and 169E139, respectively. Resource availability resulted in samples collected at 6, 12, 24, 48 and 72 hpi being pooled for each interaction prior to processing for GeneChip hybridization. Although pooling risks the loss of low-abundance transcripts and transcripts showing specific temporal expression, a general overview of the changes in defence gene transcription can still be obtained (McGrann *et al*., 2009). Transcripts of probe sets were considered to be differentially expressed if they passed the criterion of fold change (FC), relative to the mock-inoculated control, of more than two with $P < 0.05$ (Welch *T*-test). Sixty probe sets were identified as transcriptionally regulated during the Avocet*6/*Yr1* incompatible interaction, 37 of which were upregulated and 23 were downregulated (Fig. 6A; Table 1). In the compatible interaction, 42 probe sets were upregulated, whereas only one was repressed (Fig. 6A; Table 2). Functional annotation indicated that the majority of the genes in both the incompatible and compatible interactions were involved in plant defence (Fig. 6B). Closer inspection showed that, in the incompatible interaction, most of these transcripts were annotated as classical pathogenesis-related (PR) proteins, but also included transcripts involved in lignin and cell wall fortification and the defence-related oxidative burst. In the compatible interaction, the majority of defence-related transcripts were annotated as being involved in stress responses, including transcripts coding for heat shock proteins, caleosins and δ-1-pyrroline-5-carboxylate synthetase (Table 2). A number of transcripts specific to carbohydrate metabolism were also induced in the compatible interaction, in particular fructan biosynthesis (Table 2). Four probe sets were identified as common to both interactions. These transcripts were upregulated and predicted to encode for defence-related proteins, including a peroxidase, two putative chitinases and a β-1,3-glucanase (Fig. 6A; Table 3).

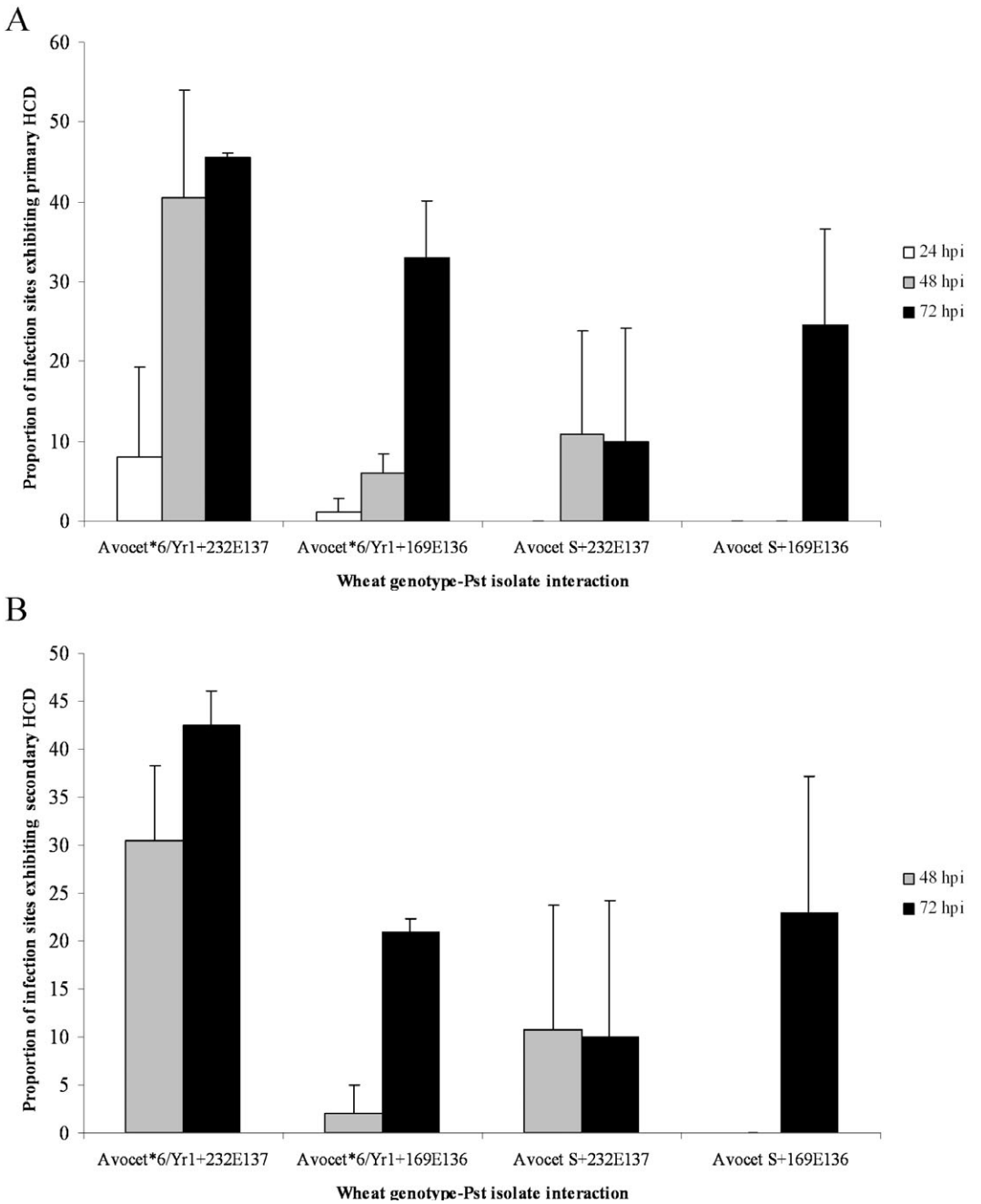


**Fig. 4** *Puccinia striiformis* f. sp. *tritici* (Pst) infection sites exhibiting mesophyll hypersensitive cell death (HCD). The percentage of infection sites exhibiting primary (A) and secondary (B) mesophyll HCD associated with Pst substomatal vesicle infection hyphae is shown for the *Yr1*-avirulent isolate 232E137 and the *Yr1*-virulent isolate 169E136 on Avocet*6/*Yr1* and Avocet S.

## Meta-analysis of *Yr*-mediated resistance transcriptomes

A meta-analysis was carried out between the *Yr1* microarray expression data and that of previously published Affymetrix wheat microarray datasets for the yellow rust race-specific *R* gene *Yr5* (Coram *et al*., 2008b) and the non-race-specific, adult plant resistance (*APR*) gene *Yr39* (Coram *et al*., 2008a). To enable a comparison to be made between *Yr1* and the published datasets, the data files for each time point analysed in the *Yr5* (6, 12, 24, 48 hpi) and *Yr39* (12, 24, 48 hpi) studies were combined and analysed as one dataset based on treat-

 

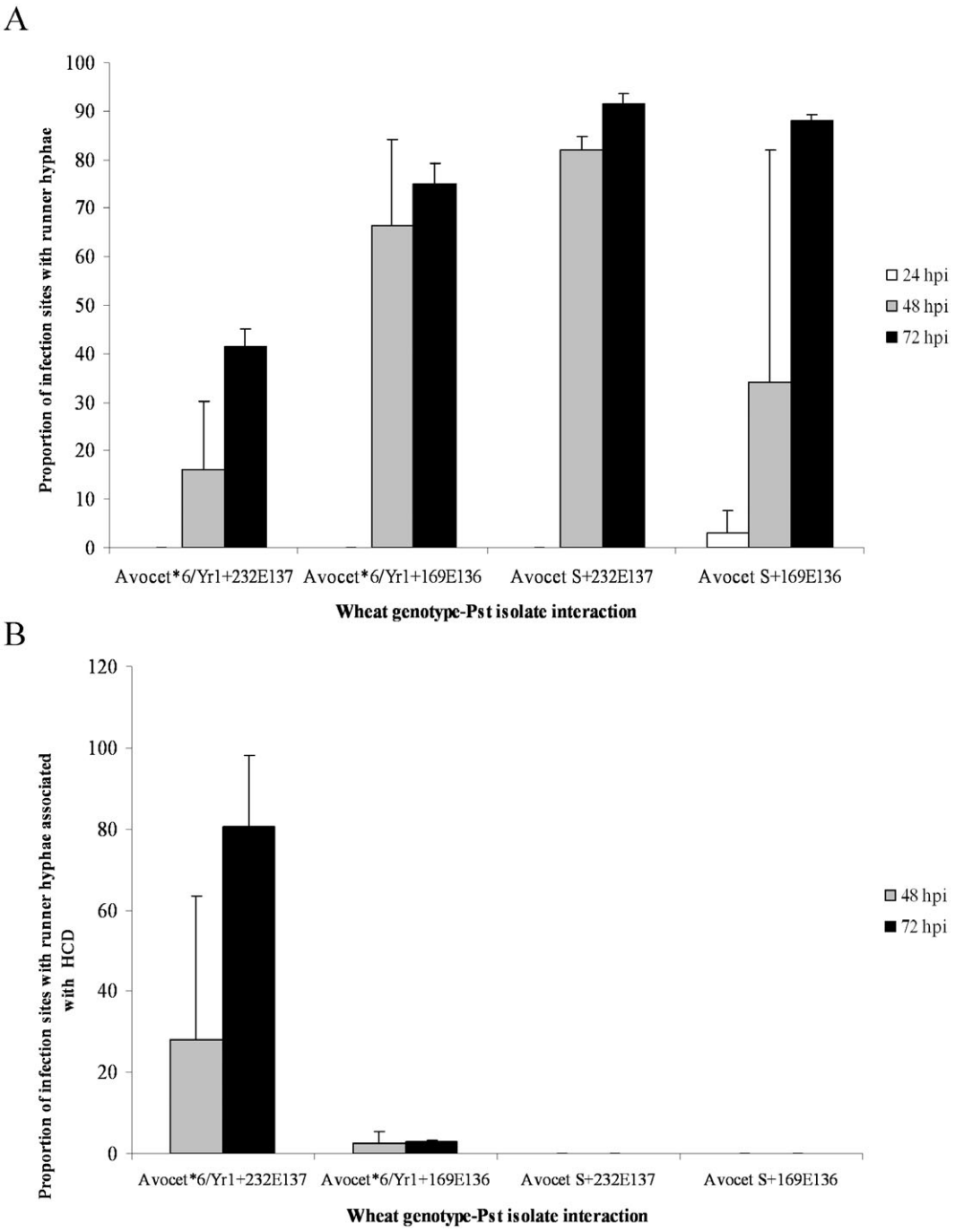


**Fig. 5** *Puccinia striiformis* f. sp. *tritici* (Pst) infection sites with runner hyphae. The percentage of infection sites having formed runner hyphae (A) and the percentage of infection sites with runner hyphae associated with hypersensitive cell death (HCD) (B) are shown for the *Yr1*-avirulent isolate 232E137 and the *Yr1*-virulent isolate 169E136 on Avocet*6/*Yr1* and Avocet S.

ment, thereby accommodating the RNA pooling method used for *Yr1*. Probe sets differentially expressed in each *R* gene-mediated interaction were identified by pair-wise comparison between pathogen-treated and mock-inoculated control samples.

Eighty and 58 probe sets were identified as specifically differentially expressed (FC > 2, $P < 0.05$, Welch *T*-test) in the *Yr1*-mediated resistant and susceptible interactions, respectively (Tables S2 and S3, see Supporting Information), significantly more than identified in the analysis of the *Yr1*

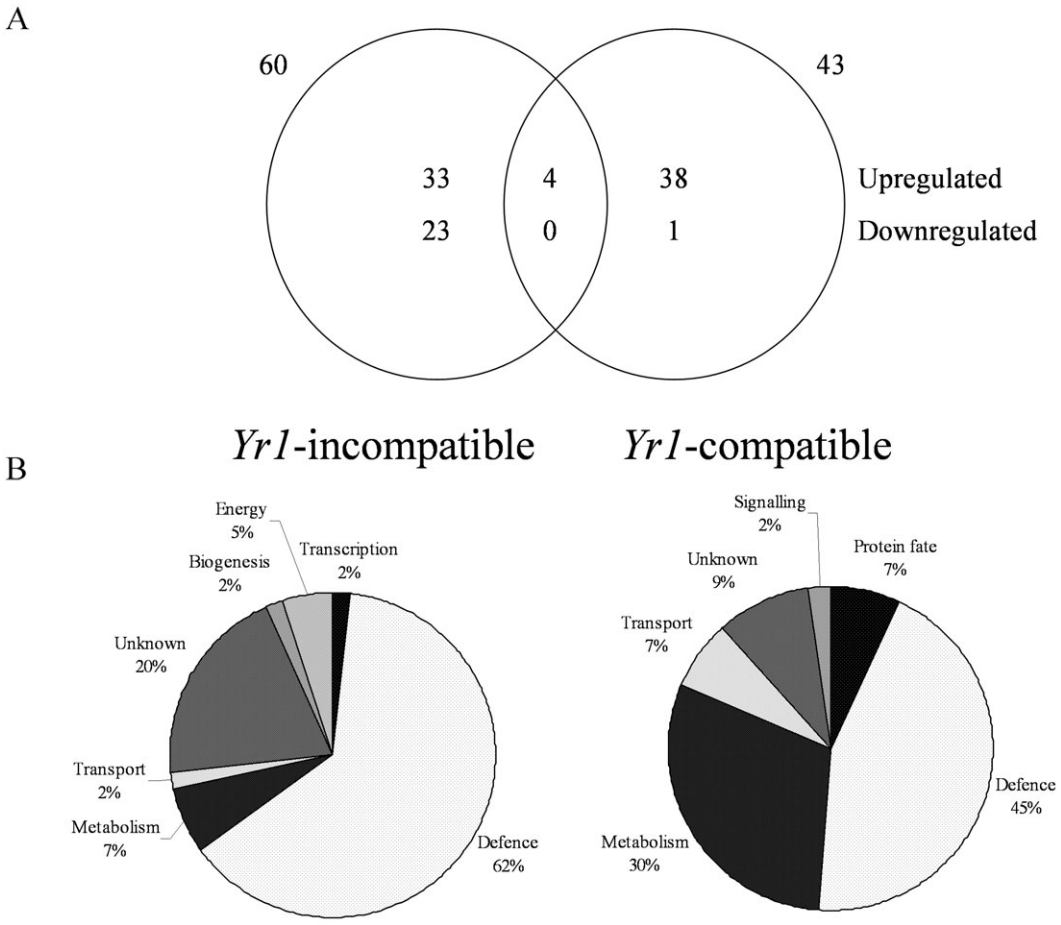


**Fig. 6** Overlap between (A) and functional classification of (B) differentially expressed probe sets that were upregulated or downregulated in the incompatible and compatible interactions between Avocet*6/*Yr1* and the *Puccinia striiformis* f. sp. *tritici Yr1*-avirulent isolate 232E137 and the *Yr1*-virulent isolate 169E136, respectively.

microarray data alone (Tables 1 and 2). The meta-analysis also identified seven transcripts that were differentially transcribed in both interactions (Table S4, see Supporting Information). Comparison of the transcriptomes regulated by the three *R* genes showed low levels of similarity (Table 4). The highest levels of conservation were observed between the transcriptomes regulated by the two race-specific *R* genes *Yr1* and *Yr5*, which shared 20 transcripts in common, all of which were upregulated. Ten of these transcripts were annotated as *PR* genes, including *PR1*, β-1,3-glucanases, peroxidases and chitinases. In addition, *WIR1*, cytokinin-*O*-glucosyltransferases, a cytochrome P450 and genes with no functional annotation were upregulated in common. The *Yr1*- and *Yr39*-regulated transcriptomes only had four probe sets in common, encoding for *PR1* and a cytokinin-*O*-glucosyltransferase transcript, all of which were in common with the *Yr5*-regulated transcriptome (Table 4).

## Quantitative reverse transcriptase-polymerase chain reaction (qRT-PCR) validation analysis of selected transcripts

Six differentially expressed probe sets functionally annotated to be involved in plant defence were selected for qRT-PCR analysis. Five of these transcripts were predicted by the microarray to be induced during the *Yr1* incompatible interaction. These included *PR2*, a β-1,3-glucanase (probe set Ta.28.1.S1_at), *PR4*, a chitin-binding protein (probe set TaAffx.108556.1.S1_at), *PR10*, a ribonuclease-like protein (probe set Ta.22619.1.S1_x_at), and two *WIR1* transcripts (probe sets Ta.97.1.S1_at and Ta.21556.1.S1_at). The sixth probe set, a *PR9* peroxidase (probe set Ta.5385.1.S1_at), was induced in response to both isolates (Fig. 7). To compare the transcription profiles with plant cellular defence responses, the six probe sets were analysed in the same four wheat–isolate inoculations as used for the

 

**Table 1** Differentially transcribed probe sets identified specifically during the incompatible interaction of *Puccinia striiformis* f. sp. *tritici* race 232E137 with Avocet 6*/*Yr1*.

| Functional category | Probe set ID | Annotation | Fold change (FC) |
|---|---|---|---|
| Defence | | | |
| Defence, cell wall | Ta.97.1.S1_at | WIR1B protein | 2.6 |
| Defence, cell wall | Ta.97.2.S1_x_at | WIR1A protein | 3.7 |
| Defence, cell wall | Ta.13.1.S1_at | WIR1 protein | 2.5 |
| Defence, cell wall | Ta.21556.1.S1_at | Pathogen-induced WIR1B protein | 5.1 |
| Defence, cell wall | Ta.21556.1.S1_x_at | Pathogen-induced WIR1B protein | 4.7 |
| Defence, cell wall | Ta.29365.1.S1_x_at | Proline-rich protein precursor | –2.0 |
| Defence, cell wall | Ta.28437.2.S1_s_at | Proline-rich protein | –4.3 |
| Defence, cell wall | Ta.21385.1.S1_x_at | Proline-rich protein | –2.5 |
| Defence, cell wall | Ta.28136.1.S1_x_at | Proline-rich protein | –3.3 |
| Defence, cell wall | Ta.24110.1.A1_s_at | Putative proline-rich protein | –3.6 |
| Defence, cell wall | Ta.30144.1.A1_x_at | Proline-rich protein | –4.7 |
| Defence, lignin | Ta.7883.1.S1_x_at | Dirigent-like protein | –2.1 |
| Defence, oxidative stress/burst | Ta.5557.1.S1_x_at | Germin-like protein | –2.5 |
| Defence, oxidative stress/burst | Ta.9599.1.S1_a_at | Glutathione-*S*-transferase | –4.5 |
| Defence, PR | Ta.28.1.S1_at | Glucan endo-1,3-β-D-glucosidase | 4.3 |
| Defence, PR | Ta.655.2.A1_x_at | prx10 peroxidase-like protein | –2.8 |
| Defence, PR | Ta.30501.1.S1_at | Chitinase II | 2.4 |
| Defence, PR | Ta.27762.1.S1_x_at | Pathogenesis-related protein 1A/1B | 5.4 |
| Defence, PR | Ta.24501.1.S1_at | Pathogenesis-related protein 1A/1B | 8.4 |
| Defence, PR | TaAffx.110196.1.S1_s_at | β-1,3-Glucanase | 2.1 |
| Defence, PR | TaAffx.108556.1.S1_at | Pathogenesis-related protein 4 | 3.5 |
| Defence, PR | TaAffx.108556.1.S1_x_at | Pathogenesis-related protein 4 | 3.3 |
| Defence, PR | Ta.25053.1.S1_at | Thaumatin-like protein (PR5) | 2.0 |
| Defence, PR | Ta.23322.3.S1_at | Thaumatin-like protein TLP8 | 4.2 |
| Defence, PR | Ta.278.1.S1_at | Pathogenesis-related protein PRB1-2 precursor | 3.2 |
| Defence, PR | Ta.278.1.S1_x_at | Pathogenesis-related protein PRB1-2 precursor | 3.2 |
| Defence, PR | Ta.62.1.S1_x_at | Pathogenesis-related protein PRB1-3 precursor | 6.2 |
| Defence, PR | Ta.22619.1.S1_x_at | Pathogenesis-related protein 10 | 2.1 |
| Defence, PR | Ta.21348.2.S1_at | Sulphur-rich/thionin-like protein | 6.2 |
| Defence, stress induced | Ta.191.1.S1_at | Thiol protease | 5.1 |
| Defence, stress induced | Ta.7479.1.S1_a_at | pTACR7 Cold-regulated protein BLT14 | –2.3 |
| Defence, stress induced | Ta.7479.2.S1_x_at | pTACR7 Cold-regulated protein BLT14 | –2.3 |
| Defence, stress induced | Ta.20658.1.S1_a_at | Putative esterase | –2.2 |
| Defence, stress induced | Ta.9110.1.S1_at | One helix protein | 2.3 |
| Biogenesis of cellular components | | | |
| Biogenesis, cell wall | Ta.23400.1.S1_at | Putative pectinacetylesterase | –2.0 |
| Energy | | | |
| Energy, electron transport | Ta.22615.1.S1_at | Cytochrome P450 | 2.2 |
| Energy, electron transport | Ta.8447.1.S1_a_at | Cytochrome P450 family protein | 2.2 |
| Energy, photosynthesis | Ta.881.2.S1_at | Putative light-harvesting chlorophyll-*a*/*b* protein of photosystem I | 2.6 |
| Metabolism | | | |
| Metabolism, secondary metabolism | Ta.23031.1.A1_at | Putative chalcone synthase 1 | –2.6 |
| Metabolism, secondary metabolism | Ta.23031.1.A1_x_at | Putative chalcone synthase 1 | –2.2 |
| Metabolism, secondary metabolism | Ta.30731.1.S1_at | Cytokinin-*O*-glucosyltransferase 1 | 2.2 |
| Metabolism, secondary metabolism | Ta.23340.1.S1_at | Cytokinin-*O*-glucosyltransferase 3 | 3.5 |
| Transcription | | | |
| Transcription, transcriptional control | Ta.14442.1.S1_at | Hap5-like protein | –2.7 |
| Transport | | | |
| Transport, endomembrane transport | Ta.9347.1.S1_s_at | Membrane protein | –2.1 |
| Function unknown | | | |
| Unknown | Ta.23297.1.S1_x_at | Hypothetical protein | –2.5 |
| Unknown | Ta.12035.1.S1_at | Hypothetical protein | 2.1 |
| Unknown | Ta.21340.1.S1_a_at | Hypothetical protein | 2.4 |
| Unknown | Ta.22662.1.S1_at | Unknown protein | 2.2 |
| Unknown | Ta.23327.1.S1_at | None | 4.5 |
| Unknown | Ta.1227.1.A1_at | None | –3.4 |
| Unknown | Ta.12127.1.A1_at | Hypothetical protein | 2.2 |
| Unknown | Ta.21314.1.S1_at | None | 2.0 |
| Unknown | TaAffx.85782.1.S1_at | Hypothetical protein | –3.8 |
| Unknown | Ta.22802.2.A1_x_at | None | –2.1 |
| Unknown | Ta.23340.2.S1_at | None | 2.7 |
| Unknown | TaAffx.15045.1.S1_at | None | –3.0 |

PR, pathogenesis-related.

**Table 2** Differentially transcribed probe sets identified specifically in the compatible interaction of *Puccinia striiformis* f. sp. *tritici* race 169E136 with Avocet 6*/*Yr1*.

| Functional category | Probe set ID | Annotation | Fold change (FC) |
|---|---|---|---|
| Defence | | | |
| Defence, cell wall | TaAffx.128643.2.A1_at | Proline-rich protein precursor | −2.0 |
| Defence, oxidative stress/burst | TaAffx.104812.1.S1_s_at | Lipoxygenase 2.1, chloroplast precursor | 2.1 |
| Defence, oxidative stress/burst | TaAffx.90316.1.S1_at | Lipoxygenase | 2.2 |
| Defence, stress induced | Ta.5610.1.S1_at | Non-symbiotic haemoglobin | 2.3 |
| Defence, stress induced | Ta.7091.1.S1_at | δ-1-pyrroline-5-carboxylate synthetase | 2.2 |
| Defence, stress induced | Ta.21547.1.S1_at | 10-kDa chaperonin | 2.2 |
| Defence, stress induced | Ta.21547.1.S1_x_at | 10-kDa chaperonin | 2.1 |
| Defence, stress induced | Ta.9830.1.A1_a_at | Putative caleosin | 3.1 |
| Defence, stress induced | Ta.9830.1.A1_at | Putative caleosin | 2.8 |
| Defence, stress induced | Ta.28631.1.S1_at | 16.9-kDa class I heat shock protein | 3.2 |
| Defence, stress induced | Ta.9377.1.S1_at | Heat shock protein precursor | 2.2 |
| Defence, stress induced | Ta.30802.1.A1_at | Heat shock 70-kDa protein | 2.1 |
| Defence, stress induced | Ta.30802.1.A1_x_at | Heat shock 70-kDa protein | 2.0 |
| Defence, stress induced | Ta.9925.1.A1_a_at | Aldehyde dehydrogenase | 2.1 |
| Defence, lignin | Ta.2659.1.S1_at | Cinnamyl alcohol dehydrogenase | 2.6 |
| Signal transduction | | | |
| Signal transduction, regulation | Ta.12348.1.A1_at | Protein phosphatase 2C | 2.2 |
| Metabolism | | | |
| Metabolism, fatty acid metabolism | Ta.6247.2.S1_at | Acetyl-CoA C-acyltransferase | 2.6 |
| Metabolism, general | Ta.14087.1.S1_at | Putative oxidoreductase | 2.1 |
| Metabolism, vitamin metabolism | Ta.22443.1.S1_s_at | Thiamine biosynthesis protein thiC | 2.2 |
| Metabolism, carbohydrate | Ta.2788.1.A1_at | Sucrose:sucrose 1-fructosyltransferase | 2.3 |
| Metabolism, carbohydrate | Ta.2789.1.S1_a_at | Sucrose:fructan 6-fructosyltransferase | 3.8 |
| Metabolism, carbohydrate | Ta.2789.2.S1_at | Sucrose:fructan 6-fructosyltransferase | 2.9 |
| Metabolism, carbohydrate | Ta.2789.2.S1_x_at | Sucrose:fructan 6-fructosyltransferase | 3.2 |
| Metabolism, carbohydrate | Ta.93.1.S1_at | Sucrose synthase 2 | 2.3 |
| Metabolism, carbohydrate | Ta.1279.1.S1_at | α-1,4-Glucan phosphorylase L isozyme | 2.0 |
| Metabolism, carbohydrate | Ta.6869.1.S1_at | ADP-glucose pyrophosphorylase small subunit | 2.2 |
| Metabolism, carbohydrate | Ta.3475.1.A1_at | Fructan 1-fructosyltransferase | 4.1 |
| Metabolism, carbohydrate | Ta.3475.2.S1_at | Fructan 1-fructosyltransferase | 4.2 |
| Metabolism, secondary metabolism | Ta.21020.1.S1_at | 2-Oxoglutarate-dependent dioxygenase | 2.2 |
| Protein fate | | | |
| Protein fate, processing | Ta.30798.3.S1_at | Asparaginyl endopeptidase | 2.0 |
| Protein fate, folding | Ta.74.1.S1_at | Protein disulphide isomerase 2 precursor | 2.7 |
| Protein fate, ubiquitination pathway | Ta.1274.1.S1_a_at | Calcyclin-binding protein | 2.1 |
| Transport | | | |
| Transport, heavy metal ion transport | Ta.11265.1.S1_at | Copper chaperone (CCH)-related protein-like | 2.3 |
| Transport, heavy metal ion transport | Ta.7567.1.A1_at | Copper chaperone (CCH)-related protein-like | 3.4 |
| Transport, vacuolar/lysosomal transport | Ta.13370.1.A1_at | Vacuolar sorting receptor 1 | 2.3 |
| Function unknown | | | |
| Unknown | Ta.25449.1.S1_s_at | Hypothetical protein | 2.2 |
| Unknown | Ta.15894.1.S1_at | None | 2.0 |
| Unknown | TaAffx.86018.1.S1_at | None | 2.3 |
| Unknown | Ta.13650.2.S1_at | None | 2.3 |

**Table 3** Probe sets differentially transcribed in both incompatible and compatible interactions of *Puccinia striiformis* f. sp. *tritici*, races 232E137 and 169E136, respectively, with Avocet 6**Yr1*.

| Functional category | Probe set ID | Annotation | Fold change (FC) | |
|---|---|---|---|---|
| | | | Incompatible | Compatible |
| Defence | | | | |
| Defence, PR | Ta.5385.1.S1_at | Peroxidase | 2.9 | 2.3 |
| Defence, PR | Ta.21342.1.S1_x_at | Chitinase | 3.6 | 2.4 |
| Defence, PR | Ta.14946.1.S1_at | Putative chitinase | 4.2 | 2.5 |
| Defence, PR | TaAffx.15327.1.S1_at | β-1,3-Glucanase (PR-2) | 8.5 | 2.4 |

PR, pathogenesis-related.

 

**Table 4** Probe sets regulated in common by *Yr1*-, *Yr5*- and *Yr39*-mediated resistance.

| Functional category | Probe set ID | Annotation | Fold change (FC)* | | |
|---|---|---|---|---|---|
| | | | *Yr1* | *Yr5* | *Yr39* |
| Defence | | | | | |
| Defence, PR | Ta.21342.1.S1_x_at | Chitinase | 3.3 | 3.1 | |
| Defence, PR | Ta.24501.1.S1_at | Pathogenesis-related protein 1A/1B | 10.8 | 4.3 | |
| Defence, PR | Ta.27762.1.S1_x_at | Pathogenesis-related protein 1A/1B | 6.5 | 2.4 | |
| Defence, PR | Ta.278.1.S1_at | Pathogenesis-related protein PRB1-2 precursor | 3.6 | 2.1 | 2.6 |
| Defence, PR | Ta.278.1.S1_x_at | Pathogenesis-related protein PRB1-2 precursor | 4.0 | 2.2 | 2.5 |
| Defence, PR | Ta.28.1.S1_at | PR2-Glucan endo-1,3-β-D-glucosidase | 3.9 | 2.5 | |
| Defence, PR | Ta.30501.1.S1_at | Chitinase II | 2.7 | 3.5 | |
| Defence, PR | Ta.5385.1.S1_at | Peroxidase | 3.5 | 4.6 | |
| Defence, PR | Ta.62.1.S1_x_at | Pathogenesis-related protein PRB1-3 precursor | 8.5 | 4.6 | 2.5 |
| Defence, PR | TaAffx.15327.1.S1_at | PR-2-β-1,3-glucanase | 9.8 | 4.9 | |
| Defence, cell wall | Ta.21556.1.S1_at | Pathogen-induced WIR1B protein | 5.8 | 4.2 | |
| Defence, cell wall | Ta.21556.1.S1_x_at | Pathogen-induced WIR1B protein | 5.7 | 4.4 | |
| Defence, cell wall | Ta.3133.1.S1_x_at | Pathogen-induced protein WIR1A homologue | 4.2 | 4.0 | |
| Defence, cell wall | Ta.97.1.S1_at | Pathogen-induced WIR1B protein | 2.7 | 3.4 | |
| Defence, cell wall | Ta.97.2.S1_x_at | Pathogen-induced WIR1A protein | 5.2 | 4.5 | |
| Metabolism | | | | | |
| Metabolism, secondary metabolism | Ta.23340.1.S1_at | Cytokinin-*O*-glucosyltransferase 3 | 4.7 | 7.0 | |
| Metabolism, secondary metabolism | Ta.30731.1.S1_at | Cytokinin-*O*-glucosyltransferase 1 | 2.1 | 5.6 | 2.4 |
| Energy | | | | | |
| Energy, electron transport | Ta.8447.1.S1_a_at | Cytochrome P450 family protein | 2.7 | 5.6 | |
| Function unknown | | | | | |
| Unknown | Ta.23340.2.S1_at | None | 3.1 | 5.9 | |
| Unknown | Ta.5518.1.S1_at | None | 3.9 | 4.2 | |

PR, pathogenesis-related.

*FC relative to mock inoculated control.

histopathological study. Statistical analysis confirmed that, for all transcripts tested, no significant differences between qRT-PCR replications were detected.

In general, all six transcripts were present at higher levels in the incompatible interaction from 24 hpi onwards, with transcript levels being significantly upregulated at 72 hpi between the incompatible and the three compatible interactions (*t*-test probabilities between 0.09 and <0.001). In the compatible interactions, the transcript levels of *PR2* and *PR4* were particularly low at all time points; however, higher levels of *PR9*, *PR10* and *WIR1* transcripts were seen between 24 and 48 hpi with isolate 232E137 (Fig. 7).

In addition, the transcription of three probe sets predicted by the meta-analysis to be induced in *Yr1*-mediated resistance, that were not identified in the original analysis, were analysed by qRT-PCR. The three transcripts examined were Ta.3976.1.S1_at (a flavanone 3-hydroxylase-like protein), Ta.3133.1.S1_x_at (a pathogen-induced protein *WIR1A* homologue) and Ta.5518.1.S1_at (function unknown). qRT-PCR analysis indicated that all three transcripts were differentially upregulated in the *Yr1*-mediated incompatible interaction. The transcript profiles were similar to those of the six probe sets obtained from the *Yr1* analysis. Transcript levels were slightly higher in the *Yr1* incompatible interaction from 24 to 48 hpi, but significantly higher at 72 hpi (*t*-test probabilities between 0.009 and <0.001; Fig. S1, see Supporting Information).

## DISCUSSION

An early and extensive HCD response was seen in the *Yr1*-mediated incompatible interaction. However, the HCD response was not exclusive to the incompatible interaction; both primary and secondary HCD were found to be associated with the initial stages of infection in all three compatible interactions (Fig. 4). HCD triggered by substomatal infection hyphae may be part of an early basal response towards both incompatible and compatible *P. striiformis* f. sp. *tritici* isolates. Runner hyphae associated with HCD were seen primarily only in the resistant interaction at 48 hpi and are presumably part of the *R* gene response mediated by *Yr1* (Fig. 5).

Both *P. striiformis* f. sp. *tritici* isolates developed at the same rate *in planta*. However, the *Yr1*-avirulent isolate 232E137 formed fewer infection sites compared with the virulent isolate 169E136 (Fig. 3), an observation that was obtained after microarray analysis had been carried out. This indicates a greater ability of race 169E136 to locate stomatal openings, form substomatal vesicles and establish infection sites. The more aggressive nature of race 169E136 was also reflected in the transcript

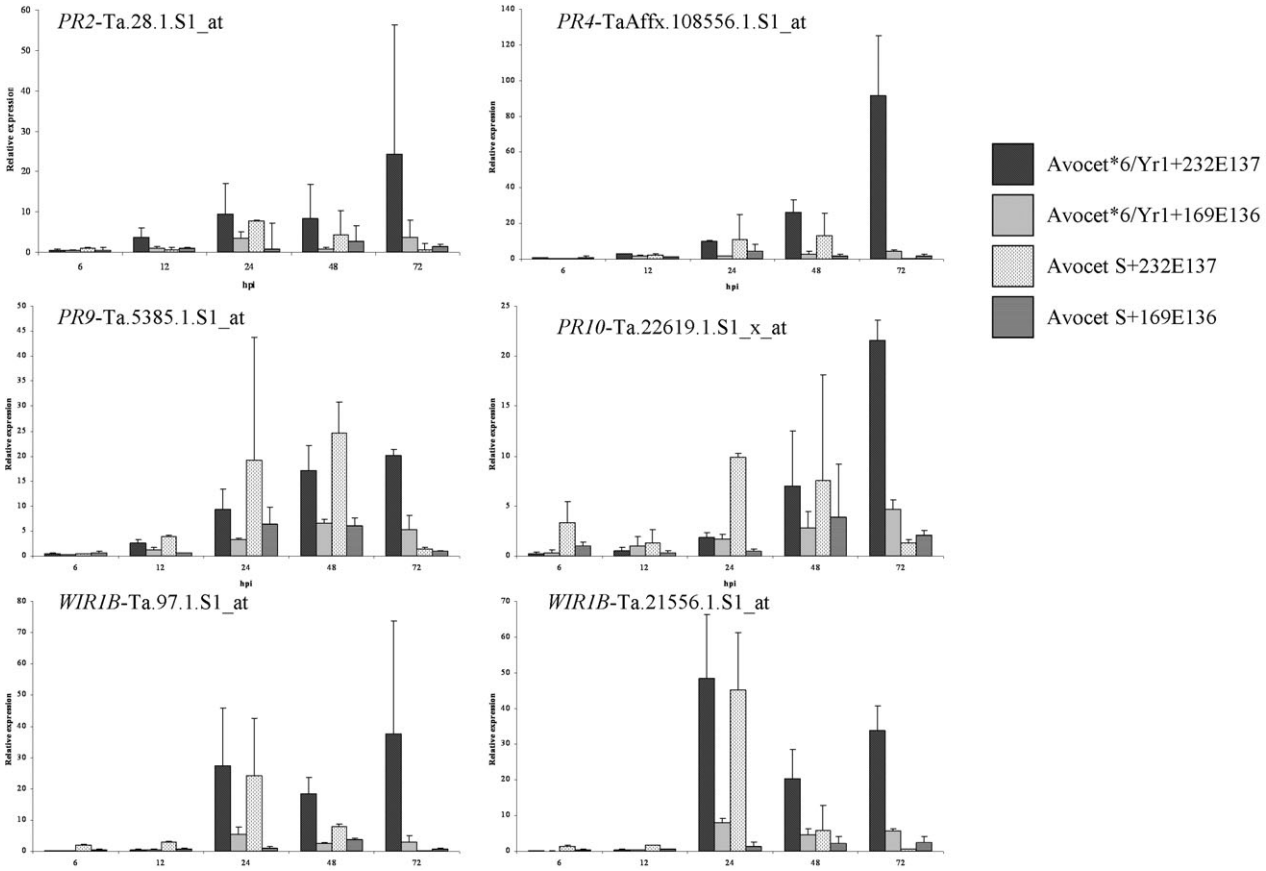


**Fig. 7** Quantitative reverse transcriptase-polymerase chain reaction (qRT-PCR) time-course validation of selected array transcripts. Six differentially expressed probe sets functionally annotated to be involved in plant defence were selected for qRT-PCR analysis. Relative transcript levels are shown for the interactions between Avocet*6/*Yr1* and Avocet S with the *Yr1*-avirulent isolate 232E137 and the *Yr1*-virulent isolate 169E136. Transcripts analysed were PR2 (a β-1,3-glucanase; probe set Ta.28.1.S1_at), PR4 (a chitin-binding protein; probe set TaAffx.108556.1.S1_at), PR9 (a peroxidase; probe set Ta.5385.1.S1_at), PR10 (a ribonuclease-like protein; probe set Ta.22619.1.S1_x_at), and two probe sets annotated as *WIR1* transcripts (Ta.97.1.S1_at and Ta21556.1.S1_at). Mean values of two independent technical replications are shown with standard deviations.

levels. Defence gene transcript levels in the compatible interactions involving 169E136 were generally lower at the mid-range time points than in the compatible interaction involving race 232E237 (Fig. 7). This may indicate a greater capacity of 169E136 to suppress early basal defence responses, resulting in its greater ability to establish infection sites and the earlier appearance of runner hyphae in the Avocet S + 169E136 compatible interaction. Alternatively, race 169E136 may trigger a weaker PTI response, resulting in a more aggressive phenotype. Either way, this did not appear to affect the overall infection phenotype observed at 14 dpi (Fig. 1). Having formed an infection site, both isolates were able to establish multiple runner hyphae, leading to comparable levels of pustule and urediniospore formation in all compatible interactions.

In the microarray analysis, probe sets differentially transcribed specifically in the incompatible interaction can be inferred to be involved in *Yr1*-mediated resistance, whereas those specific to the compatible interaction may be recruited by *P. striiformis* f. sp. *tritici* for the establishment of infection, or may be involved in the plant's response to pathogen colonization. Transcripts exhibiting similar expression profiles in response to avirulent and virulent *P. striiformis* f. sp. *tritici* isolates are considered to be part of the basal resistance response (Coram *et al*., 2008b). qRT-PCR validation of selected probe sets showed no significant induction of transcription of the *Yr1*-specific defence transcripts before 24 hpi (Fig. 7), but demonstrated significantly higher transcript levels at 72 hpi in the incompatible interaction. This may indicate a limited role for these particular transcripts in the HCD response seen towards substomatal infection hyphae at 24 hpi (Fig. 4), but a possible role in *Yr1*-mediated HCD resistance (Fig. 5).

A high proportion of the defence-related transcripts identified in the *Yr1*-mediated incompatible interaction were annotated as *PR*-like genes (Table 1). The induction of *PR* transcripts appears

 

to be a common response of wheat to plant pathogens (Adhikari *et al*., 2009; Bolton *et al*., 2008; Coram *et al*., 2008a, b, 2010; Hulbert *et al*., 2007; Moldenhauer *et al*., 2008; Tufan *et al*., 2009). There were also a number of transcripts specific to the incompatible interaction with putative roles in plant cell wall defence, including proline-rich and dirigent-like proteins. Proline-rich proteins have been identified that assist cell wall strengthening through cross-linking mechanisms (Sheng *et al*., 1991; Zhang *et al*., 1993), whereas dirigent proteins are involved in lignin biosynthesis (Burlat *et al*., 2001; Davin and Lewis, 2005). Transcripts of both of these proteins were downregulated in the *Yr1* incompatible interaction, which may indicate a transcriptional feedback regulation mechanism operating for these genes. Transcripts of *WIR1* were also commonly upregulated in the *Yr1*-mediated incompatible interaction. *WIR1*-like transcripts have been shown to be induced in wheat in response to both biotrophic and necrotrophic pathogens (Bolton *et al*., 2008; Bull *et al*., 1992; Coram *et al*., 2008a, b, 2010; Desmond *et al*., 2008; Hulbert *et al*., 2007; Tufan *et al*., 2009). *WIR1* is a small membrane-associated protein with a proposed role in maintaining plasma membrane cell wall integrity (Bull *et al*., 1992), possibly preventing excessive cell damage in regions undergoing an HCD response. *WIR1* may therefore have a role in limiting the damage done by the extensive, cell-to-cell HCD response seen in the incompatible interaction. Furthermore, two probe sets encoding cytokinin-*O*-glucosyltransferases (Ta.30731.1.S1_at and Ta.23340.1.S1_at) were also found to be induced in the *Yr1*-mediated incompatible interaction. Glucosyltransferases are involved in the regulation of cellular homeostasis and secondary metabolism, and have been shown to protect host cells by detoxifying pathogen toxins (Poppenberger *et al*., 2003). Ta.30731.1.S1_at and Ta.23340.1.S1_at were also found to be induced in response to *Magnaporthe oryzae* (Tufan *et al*., 2009) and *Fusarium pseudograminearum* (Desmond *et al*., 2008), suggesting a possible common detoxification pathway in wheat against fungal pathogens.

Of the probe sets upregulated in the compatible interaction, nine were involved in processes relating to carbohydrate metabolism, in particular fructan biosynthesis. As *P. striiformis* f. sp. *tritici* is a biotrophic pathogen, it needs to acquire nutrients from the living plant for fungal growth; the induction of these transcripts could therefore indicate a shift in host metabolism that is required for fungal development. The reprogramming of carbohydrate metabolism has been reported in other plant–pathogen interactions. *Sclerotinia sclerotiorum* infection in *Brassica* species altered the expression of genes encoding for enzymes involved in carbohydrate and energy metabolism, redirecting carbon reserves to the tricarboxylic acid cycle (Zhao *et al*., 2009). In maize, *Ustilago maydis* colonization prevents the establishment of C4 photosynthesis (Horst *et al*., 2008). The changes in carbohydrate metabolism in infected leaves suggest that the fungus prevents the leaf from establishing a sink to sources transition, maintaining sink metabolism in the infected plant cells for fungal growth.

To compare the *Yr1*-regulated transcriptome with that of previously published datasets for *Yr*-mediated *P. striiformis* f. sp. *tritici*–wheat interactions, a meta-analysis of the array data was performed (Table 4). Comparison of the transcriptomes regulated by *Yr1*, *Yr5* and *Yr39* showed low similarity, with the two race-specific *R* genes *Yr1* and *Yr5* having the most differentially expressed transcripts in common. All of the annotated transcripts, except one (cytochrome P450 family protein), encode for defence-related genes, including classic *PR* genes, genes involved in fungal detoxification and cell wall remodelling. A similar lack of commonality in transcript profiles was observed in a meta-analysis of *Yr R* gene-mediated resistance using a custom-array, most of the transcripts showing common differential expression between *Yr* genes representing classic *PR* and defence-related genes (Coram *et al*., 2010).

This study has demonstrated that resistance mediated by the race-specific *R* gene *Yr1* against *P. striiformis* f. sp. *tritici* in wheat involves two phases of HCD. The first phase targets initial fungal invasion and occurs in both incompatible and compatible interactions. The second phase targets those infection sites that have escaped the first HCD response and is strongly associated with *Yr1*-mediated resistance. Transcription profiling of the *Yr1*-mediated interaction indicated that the second phase of HCD is accompanied by an increase in transcript abundance of classic plant defence-related genes, whereas a meta-analysis comparison suggested that similar defence-related genes may also be important in other wheat race-specific *Yr R* gene interactions.

## EXPERIMENTAL PROCEDURES

### Plant material and *P. striiformis* f. sp. *tritici* inoculations

Avocet*6/*Yr1* was developed at the Plant Breeding Institute, Cobbitt, Sydney, Australia by backcrossing the *Yr1* donor cultivar Chinese 166 with the recurrent susceptible spring wheat selection Avocet S (Wellings *et al*., 2004). Seedlings of Avocet*6/*Yr1* and Avocet S were grown to growth stage 12–13 (Zadoks *et al*., 1974) under a 16-h/8-h photoperiod cycle, supplemented with sodium lighting (240 μmol/m$^2$/s), at day/night temperatures of 20 °C/15 °C and a relative humidity of 60% in a spore-free containment level 2 glasshouse. Seedlings were inoculated with either the *P. striiformis* f. sp. *tritici* isolate race 169E136 (virulent for *Yr1*) or race 232E137 (avirulent for *Yr1*), or with talc for the mock inoculation (Boyd and Minchin, 2001). This resulted in one incompatible (Avocet*6/*Yr1* + 232E137) and three compatible (Avocet*6/*Yr1* + 169E136,

Avocet S + 169E136 and Avocet S + 232E137) wheat–*P. striiformis* f. sp. *tritici* interactions, as well as control plant inoculations: Avocet*6/*Yr1* + talc and Avocet S + talc. Two repeat inoculation experiments were undertaken 2 weeks apart. Leaf tissue was collected at 6, 12, 24, 48 and 72 hpi for both the histopathological and qRT-PCR analyses.

### Histopathology of *P. striiformis* f. sp. *tritici*–wheat interactions

To examine *P. striiformis* f. sp. *tritici* development and subsequent plant responses during the *Yr1*-mediated incompatible and three compatible interactions, a 5-cm leaf sample was collected from four seedlings at 6, 12, 24, 48 and 72 hpi for each of the four wheat–*P. striiformis* f. sp. *tritici* interactions. Two of the leaf samples were stored at −80 °C for subsequent RNA extraction and qRT-PCR analysis. The remaining leaf samples were cleared and fixed in chloral hydrate (Garrood, 2001; Tufan *et al*., 2009). Fungal structures were stained using Uvitex-2B (Ciba-Geigy, Basle, Switzerland) following the protocol of Moldenhauer *et al*. (2006) with the modifications of Tufan *et al*. (2009). Fungal structures and plant cellular autofluorescence were examined using a Leica SP2 confocal microscope (Leica Microsystems Ltd., Milton Keynes, Buckinghamshire, UK) with a Plan-Apochromat × 40.1.25 EC Plan-Neofluar oil immersion objective lens. Spectral data were collected by excitation with 405-nm diode and 488-nm argon lasers. Uvitex-2B-stained fungal structures and autofluorescing plant cellular structures were identified using a Uvitex-2B-specific filter (420–500 nm) and an autofluorescence-specific filter (505–654 nm), respectively.

Fungal development and associated plant responses were classified into the following developmental stages: (i) successful *P. striiformis* f. sp. *tritici* infection sites were classified as the development of a substomatal vesicle within the stomatal cavity; infection sites were measured relative to the number of germinated urediniospores; (ii) the development of *P. striiformis* f. sp. *tritici* infection and of runner hyphae was measured relative to the number of successful infection sites; (iii) plant primary hypersensitive cell death (1° HCD) was classified as a plant cell exhibiting autofluorescence that was in direct physical contact with a substomatal vesicle infection hypha; (iv) plant secondary hypersensitive cell death (2° HCD) was classified as a plant cell exhibiting autofluorescence that was not in direct physical contact with an infection hypha, but adjacent to a plant cell that was exhibiting autofluorescence; infection sites exhibiting 1° and 2° HCD were measured relative to the total number of successful infection sites; (v) runner hyphae associated with plant HCD were measured relative to the number of infection sites that had formed runner hyphae; between 50 and 200 infection sites were observed per leaf sample.

### Affymetrix wheat genome array GeneChip® transcriptome analysis

Three Avocet*6/*Yr1* inoculations were performed independent to those described for the histopathological and qRT-PCR analyses. A single genotype, carrying the race-specific yellow rust *R* gene *Yr1*, was used so as to avoid host genetic variation caused by incomplete isogenicity (Coram *et al*., 2008b). Forty seedlings of Avocet*6/*Yr1* were inoculated with *P. striiformis* f. sp. *tritici* race 232E137 or 169E136, or a mock inoculation. Three biological replications were inoculated independently and all nine trays of seedlings (three biological replicates × avirulent + virulent + mock) were randomized in the glasshouse after inoculation. Six seedlings were collected for RNA extraction at 6, 12, 24, 48 and 72 hpi. The remaining seedlings were left to monitor the yellow rust infection phenotype at 14 dpi.

RNA was isolated using the TRIzol reagent method, following the manufacturer's instructions (Invitrogen, Carlsbad, CA, USA). Equal amounts of total RNA from each time point (16 μg) were pooled to obtain 80 μg of total RNA for each treatment (232E137, 169E136 and mock inoculations). Pooled RNA samples were further purified using the Qiagen RNeasy mini-kit according to the manufacturer's instructions (Qiagen, Hilden, Germany), and RNA integrity was confirmed using the Agilent 2100 Bioanalyzer (Agilent Technologies, Stockport, UK).

The Wheat GeneChip, containing 61 127 probe sets representing 55 052 transcripts, was used to investigate transcriptional changes in each wheat–*P. striiformis* f. sp. *tritici* interaction (Affymetrix, Santa Clara, CA, USA; http://www.affymetrix.com/estore/browse/products.jsp?navMode=34000&productId=131517&navAction=jump&aId=productsNav). Each probe set was assumed to represent a single transcript. Three biological replications were examined, using the pooled RNA from the 6-, 12-, 24-, 48- and 72-hpi time points from each inoculation. Affymetrix GeneChip processing, including RNA quality control, microarray hybridization and data acquisition, was performed through contract research services by the John Innes Genome Laboratory, John Innes Centre, Norwich, UK.

Data were analysed using GeneSpring GX10 (Agilent Technologies), following Robust Multichip Average (RMA) normalization and baseline to median transformation of each data file. Two comparisons were made to identify probe sets differentially transcribed during incompatible (avirulent *P. striiformis* f. sp. *tritici* isolate 232E137 vs. mock) and compatible (virulent *P. striiformis* f. sp. *tritici* isolate 169E136 vs. mock) interactions. Probe sets with unreliable signals were discarded using the 'filter on expression' tool. Differentially expressed probe sets were selected using a Welch *T*-test ($P < 0.05$) and FC > 2. Functional annotation of differentially expressed probe sets was performed using the plant expression database (http://www.plexdb.org/modules/PD_probeset/annotation.php?genechip=Wheat) and

 

HarvEST (Affymetrix Wheat1 Chip v.1.54). Gene ontology was established using the TIGR rice genome annotation and Uniprot (http://beta.uniprot.org/) with functional classification based on the categories of Coram *et al*. (2008a, b).

### Meta-analysis comparison of wheat yellow rust resistance gene-mediated transcriptomes

Data (CEL) files from the *Yr5* (Coram *et al*., 2008b) and *Yr39* (Coram *et al*., 2008a) microarray analyses were retrieved from PLEXdb (http://www.plexdb.org/) and uploaded with the *Yr1* microarray CEL files into GeneSpring GX10. Each data file was preprocessed with RMA normalization and baseline to median transformation. CEL files for specific time points in the *Yr5* (Coram *et al*., 2008b) and *Yr39* (Coram *et al*., 2008a) analyses were combined to allow comparison with the *Yr1* dataset, where RNA from each time point was pooled prior to hybridization to the Affymetrix GeneChip. Pair-wise comparisons were made between pathogen-treated and mock-inoculated control samples (Table S1). Differentially expressed probe sets, selected using a Welch *T*-test ($P < 0.05$) and FC > 2, were compared between *Yr1* and *Yr5*, and between *Yr1* and *Yr39*.

### qRT-PCR time course analyses of selected transcripts

RNA was extracted using the RNeasy Plant Mini Kit (Qiagen) following the manufacturer's instructions. Each sample was treated with TURBO DNA-free (Ambion, Austin, TX, USA) prior to cDNA synthesis from 1 μg of total RNA using SuperScript™ III-RNase $H^-$ reverse transcriptase (Invitrogen), according to the manufacturer's recommendations. cDNA was diluted 1:20 with nuclease-free water prior to use. qRT-PCRs consisted of 10 μL Sybr Green JumpStart™ Taq Ready mix (Sigma-Aldrich, St. Louis, MO, USA), 5 μL cDNA template and 0.1 μM of forward and reverse primers in a final reaction volume of 20 μL. PCR amplification and real-time analysis were performed using the DNA engine Opticon2 Continuous Fluorescence Detector (MJ Research Inc., Alameda, CA, USA). The cycling conditions were 95 °C for 4 min, followed by 40 cycles of 30 s at 94 °C, 30 s at 60 °C and 30 s at 72 °C. Melt curve analysis was used at the end of each reaction to check primer–dimer formation and gene-specific product amplification. Data were analysed using Opticon Monitor™ analysis software v2.02 (MJ Research Inc.). Prior to expression analysis, amplification efficiencies of each primer set were calculated by standard curves using a dilution series of wheat cDNA. Only primer sets with an efficiency of more than 80% were used for qRT-PCR analysis. Three reference genes, ubiquitin (Van Riet *et al*., 2006), glyceraldehyde-3-phosphate dehydrogenase (GAPDH) and elongation factor-1α (McGrann *et al*., 2009), were used for normalization. geNorm analysis indicated that all three transcripts were stable under our experimental conditions, and was used to generate a normalization factor for each cDNA sample (geNorm program v3.5; http://medgen.ugent.be/~jvdesomp/genorm/; Vandesompele *et al*., 2002). The normalized expression of each gene of interest was calculated relative to the mock-inoculated control after normalization factor correction of ΔCT. All primer sequences used in this study are given in Table S5 (see Supporting Information). The probe sets Ta.97.1.S1_at, Ta21556.1.S1_at and Ta.3133.1.S1_x_at are predicted to encode for *WIR1* proteins. Primers were designed to specifically amplify each probe set.

### Statistical analysis

The two *P. striiformis* f. sp. *tritici* inoculation experiments carried out for the histopathological and qRT-PCR analyses were analysed independently. The histopathological examination was analysed using generalized linear mixed modelling (GLMM; Welham, 1993). A binomial distribution with a logit transformation was used to compare the proportion of infection sites relative to germinated urediniospores, the proportion of infection sites having formed infection hyphae and runner hyphae, the percentage of infection sites exhibiting 1° and 2° HCD and the percentage of infection sites with runner hyphae associated with plant HCD. The models fitted compared replicate, plant genotype, isolate and time point effects. Differences between isolates and time points significant at an *F*-value probability $P < 0.001$ were further compared by *t*-test analysis. qRT-PCR relative transcript levels were compared using general linear regression. The model fitted compared replicate tests, plant genotypes, isolates and time points, and isolate–time point interactions. Differences between isolates and time points significant at an *F*-value probability $P < 0.01$ were further compared by *t*-test analysis. All analyses were carried out using the statistical package GenStat® for Windows, 9th Edition (GenStat Release 9 Committee, 2007).

## ACKNOWLEDGEMENTS

The authors are grateful for the research grants made available to MSA from the State Planning Organization of the Republic of Turkey (DPT2004K120750), International Centre for Genetic Engineering and Biotechnology (ICGEB-CRP/TUR07-03) and Middle East Technical University (METU) research funds. We also thank Grant Calder for help with confocal microscopy. MIAME/Plant-compliant microarray data from this study have been deposited in PLEXdb (http://www.plexdb.org) with accession number TA25.

## REFERENCES

**Adhikari, T.B., Bai, J.F., Meinhardt, S.W., Gurung, S., Myrfield, M., Patel, J., Ali, S., Gudmestad, N.C. and Rasmussen, J.B.** (2009) *Tsn1-*

mediated host responses to ToxA from *Pyrenophora tritici-repentis*. *Mol. Plant–Microbe Interact.* **22**, 1056–1068.

**Bayles, R.A., Flath, K., Hövmoller, M.S. and de Vallavieille-Pope, C.** (2000) Breakdown of the *Yr17* resistance to yellow rust of wheat in northern Europe. *Agronomie*, **20**, 805–811.

**Bolton, M.D., Kolmer, J.A., Xu, W.W. and Garvin, D.F.** (2008) *Lr34*-mediated leaf rust resistance in wheat: transcript profiling reveals a high energetic demand supported by transient recruitment of multiple metabolic pathways. *Mol. Plant–Microbe Interact.* **21**, 1515–1527.

**Boyd, L.A.** (2005) Can Robigus defeat an old enemy?—Yellow rust of wheat. *J. Agric. Sci.* **143**, 233–243.

**Boyd, L.A. and Minchin, P.N.** (2001) Wheat mutants showing altered adult plant disease resistance. *Euphytica*, **122**, 361–368.

**Bull, J., Mauch, F., Hertig, C., Rebmann, G. and Dudler, R.** (1992) Sequence and expression of a wheat gene that encodes a novel protein associated with pathogen defense. *Mol. Plant–Microbe Interact.* **5**, 516–519.

**Burlat, V., Kwon, M., Davin, L.B. and Lewis, N.G.** (2001) Dirigent proteins and dirigent sites in lignifying tissues. *Phytochemistry*, **57**, 883–897.

**Caldo, R.A., Nettleton, D. and Wise, R.P.** (2004) Interaction-dependent gene expression in *Mla*-specified response to barley powdery mildew. *Plant Cell*, **16**, 2514–2528.

**Caldo, R.A., Nettleton, D., Peng, J.Q. and Wise, R.P.** (2006) Stage-specific suppression of basal defense discriminates barley plants containing fast- and delayed-acting *Mla* powdery mildew resistance alleles. *Mol. Plant–Microbe Interact.* **19**, 939–947.

**Cartwright, D.W. and Russell, G.E.** (1981) Development of *Puccinia striiformis* in a susceptible winter-wheat variety. *Trans. Br. Mycol. Soc.* **76**, 197–204.

**Chen, X.M.** (2005) Epidemiology and control of stripe rust [*Puccinia striiformis* f. sp *tritici*] on wheat. *Can. J. Plant Pathol.* **27**, 314–337.

**Coram, T.E., Settles, M.L. and Chen, X.M.** (2008a) Transcriptome analysis of high-temperature adult-plant resistance conditioned by *Yr39* during the wheat–*Puccinia striiformis* f. sp *tritici* interaction. *Mol. Plant Pathol.* **9**, 479–493.

**Coram, T.E., Wang, M.N. and Chen, X.M.** (2008b) Transcriptome analysis of the wheat–*Puccinia striiformis* f. sp *tritici* interaction. *Mol. Plant Pathol.* **9**, 157–169.

**Coram, T.E., Huang, X., Zhan, G., Settles, M.L. and Chen, X.M.** (2010) Meta-analysis of transcripts associated with race-specific resistance to stripe rust in wheat demonstrates common induction of blue copper-binding protein, heat-stress transcription factor, pathogen-induced WIR1A protein, and ent-kaurene synthase transcripts. *Funct. Integr. Genomics*. DOI: 10.1007/s10142-009-0148-5.

**Davin, L.B. and Lewis, N.G.** (2005) Lignin primary structures and dirigent sites. *Curr. Opin. Biotechnol.* **16**, 407–415.

**Desmond, O.J., Manners, J.M., Schenk, P.M., Maclean, D.J. and Kazan, K.** (2008) Gene expression analysis of the wheat response to infection by *Fusarium pseudograminearum*. *Physiol. Mol. Plant Pathol.* **73**, 40–47.

**Garrood, J.M.** (2001) The interaction of *Puccinia striiformis* with wheat and barley. PhD thesis, University of East Anglia.

**GenStat Release 9 Committee** (2007) *GenStat® for Windows Release 9.1*. Oxford, UK: VSN International.

**Horst, R.J., Engelsdorf, T., Sonnewald, U. and Voll, L.M.C.** (2008) Infection of maize leaves with *Ustilago maydis* prevents establishment of C-4 photosynthesis. *J. Plant Physiol.* **165**, 19–28.

**Hulbert, S.H., Bai, J., Fellers, J.P., Pacheco, M.G. and Bowden, R.L.** (2007) Gene expression patterns in near isogenic lines for wheat rust resistance gene *Lr34*/*Yr18*. *Phytopathology*, **97**, 1083–1093.

**Jagger, L.J.** (2009) Yellow rust resistance in wheat c.v. ALCEDO: genetic and phenotypic characterisation of a durable form of resistance. PhD thesis, University of East Anglia.

**Jones, J.D.G. and Dangl, J.L.** (2006) The plant immune system. *Nature*, **444**, 323–329.

**Lupton, F.G.H. and Macer, R.C.F.** (1962) Inheritance of resistance to yellow rust (*Puccinia glumarum* Erikss. & Henn.) in seven varieties of wheat. *Trans. Br. Mycol. Soc.* **45**, 21–45.

**Mares, D.J.** (1979) Light and electron-microscope study of the interaction of yellow rust (*Puccinia-striiformis*) with a susceptible wheat cultivar. *Ann. Bot.* **43**, 183–189.

**Mares, D.J. and Cousen, S.** (1977) Interaction of yellow rust (*Puccinia-striiformis*) with winter-wheat cultivars showing adult plant resistance – macroscopic and microscopic events associated with resistant reaction. *Physiol. Plant Pathol.* **10**, 257–274.

**McGrann, G.R.D., Townsend, B.J., Antoniw, J.F., Asher, M.J.C. and Mutasa-Göttgens, E.S.** (2009) Barley elicits a similar early basal defence response during host and non-host interactions with *Polymyxa* root parasites. *Eur. J. Plant Pathol.* **123**, 5–15.

**McIntosh, R.A., Wellings, C.R. and Park, R.F.** (1995) *Wheat Rust–An Atlas of Resistance Genes*. Canberra, Australia: CSIRO Publications.

**Melichar, J.P.E., Berry, S., Newell, C., MacCormack, R. and Boyd, L.A.** (2008) QTL identification and microphenotype characterisation of the developmentally regulated yellow rust resistance in the UK wheat cultivar Guardian. *Theor. Appl. Genet.* **117**, 391–399.

**Moldenhauer, J., Moerschbacher, B.M. and Van der Westhuizen, A.J.** (2006) Histological investigation of stripe rust (*Puccinia striiformis* f.sp *tritici*) development in resistant and susceptible wheat cultivars. *Plant Pathol.* **55**, 469–474.

**Moldenhauer, J., Pretorius, Z.A., Moerschbacher, B.M., Prins, R. and Van Der Westhuizen, A.J.** (2008) Histopathology and PR-protein markers provide insight into adult plant resistance to stripe rust of wheat. *Mol. Plant Pathol.* **9**, 137–145.

**Poppenberger, B., Berthiller, F., Lucyshyn, D., Sieberer, T., Schuhmacher, R., Krska, R., Kuchler, K., Glossl, J., Luschnig, C. and Adam, G.** (2003) Detoxification of the *Fusarium* mycotoxin deoxynivalenol by a UDP-glucosyltransferase from *Arabidopsis thaliana*. *J. Biol. Chem.* **278**, 47 905–47 914.

**Sheng, J.S., Dovidio, R. and Mehdy, M.C.** (1991) Negative and positive regulation of a novel proline-rich protein messenger-RNA by fungal elicitor and wounding. *Plant J.* **1**, 345–354.

**Tufan, H.A., McGrann, G.R.D., Magusin, A., Morel, J.-B., Miché, L. and Boyd, L.A.** (2009) Wheat Blast: histopathology and transcriptome reprogramming in response to adapted and non-adapted *Magnaporthe* isolates. *New Phytol.* **184**, 473–484.

**Van Riet, L., Nagaraj, V., Van den Ende, W., Clerens, S., Wiemken, A. and Van Laere, A.** (2006) Purification, cloning and functional characterization of a fructan 6-exohydrolase from wheat (*Triticum aestivum* L.). *J. Exp. Bot.* **57**, 213–223.

**Vandesompele, J., De Preter, K., Pattyn, F., Poppe, B., Van Roy, N., De Paepe, A. and Speleman, F.** (2002) Accurate normalization of real-time quantitative RT-PCR data by geometric averaging of multiple

 

internal control genes. *Genome Biol*. **3**, research0034.0031–research0034.0011.

**Vergne, E., Ballini, E., Marques, S., Mammar, B.S., Droc, G., Gaillard, S., Bourot, S., DeRose, R., Tharreau, D., Notteghem, J.L., Lebrun, M.H. and Morel, J.-B.** (2007) Early and specific gene expression triggered by rice resistance gene *Pi33* in response to infection by ACE1 avirulent blast fungus. *New Phytol*. **174**, 159–171.

**Welham, S.J.** (1993) Procedure GLMM. In: *GenStat 5 Procedure Library Manual Release 3 [1]* (Payne, R.W., Arnold, G.M. and Morgan, G.W., eds), pp. 187–192. Oxford, UK: Numerical Algorithms Group.

**Wellings, C.R., Singh, R.P., McIntosh, R.A. and Pretorius, Z.A.** (2004) The development and application of near isogenic lines for the wheat stripe (yellow) rust pathosystem. *11th International Cereal Rusts and Powdery Mildew Conference*. John Innes Centre, Norwich, UK, p. 39.

**Zadoks, J.C., Chang, T.T. and Konzak, C.F.** (1974) Decimal code for growth stages of cereals. *Weed Res*. **14**, 415–421.

**Zhang, S.Q., Sheng, J.S., Liu, Y.D. and Mehdy, M.C.** (1993) Fungal elicitor-induced bean proline-rich protein messenger-RNA down-regulation is due to destabilization that is transcription and translation dependent. *Plant Cell*, **5**, 1089–1099.

**Zhao, J., Buchwaldt, L., Rimmer, S.R., Sharpe, A., McGregor, L., Bekkaour, D. and Hegedus, D.** (2009) Patterns of differential gene expression in *Brassica napus* cultivars infected with *Sclerotinia sclerotiorum*. *Mol. Plant Pathol*. **10**, 635–649.

**Zipfel, C.** (2008) Pattern-recognition receptors in plant innate immunity. *Curr. Opin. Immunol*. **20**, 10–16.

## SUPPORTING INFORMATION

Additional Supporting Information may be found in the online version of this article:

**Fig. S1** Quantitative reverse transcriptase-polymerase chain reaction (qRT-PCR) time-course validation of additional transcripts identified by meta-analysis.

**Table S1** Details of microarray experiments used for meta-analysis.

**Table S2** Differentially transcribed probe sets identified specifically during the incompatible interaction of *Puccinia striiformis* f. sp. *tritici* race 232E137 with Avocet 6*/*Yr1* as identified by the meta-analysis.

**Table S3** Differentially transcribed probe sets identified specifically during the compatible interaction of *Puccinia striiformis* f. sp. *tritici* race 169E136 with Avocet 6*/*Yr1* as identified by the meta-analysis.

**Table S4** Probe sets differentially transcribed in both incompatible and compatible interactions of *Puccinia striiformis* f. sp. *tritici*, races 232E137 and 169E136, respectively, with Avocet 6**Yr1* as identified by the meta-analysis.

**Table S5** Quantitative reverse transcriptase-polymerase chain reaction (qRT-PCR) primers used in this study.

Please note: Wiley-Blackwell are not responsible for the content or functionality of any supporting materials supplied by the authors. Any queries (other than missing material) should be directed to the corresponding author for the article.